

Proceedings

# A Characterization Study of Morphology and Properties of Poly(3-hydroxybutyrate-*co*-3-hydroxyhexanoate) (PHBHHx)/Aloe Vera Fibers Biocomposites: Effect of Fiber Surface Treatments <sup>†</sup>

Celia Idres <sup>1,2,\*</sup>, Mustapha Kaci <sup>1</sup>, Nadjet Dehouche <sup>1</sup>, Idris Zembouai <sup>1</sup> and Stéphane Bruzaud <sup>2</sup>

<sup>1</sup> Laboratoire des Matériaux Polymères Avancés (LMPA), Université de Bejaia, 06000, Algeria; kacimu@yahoo.fr (M.K.); dehouche\_nadjet@yahoo.fr (N.D.); zembouaiidris@yahoo.fr (I.Z.)

<sup>2</sup> Institut de recherche Dupuy de Lôme (IRDL), UMR CNRS 6027, Université de Bretagne-Sud, Rue Saint Maudé, 56321, Lorient Cedex France; stephane.bruzaud@univ-ubs.fr

\* Correspondence: idres.celia@gmail.com; Tel.: +213-662-1586-37

† Presented at the First International Conference on “Green” Polymer Materials 2020, 5–25 November 2020; Available online: <https://cgpm2020.sciforum.net/>.

Published: date

**Abstract:** The study aims to investigate the effect of various surface treatments of Aloe Vera fibers (AVF) used as reinforcement in PHBHHx biocomposites that were prepared by melt compounding at 20 wt% of filler content. The surface fibers were modified with alkaline, organosilanes and combined alkaline/organosilanes. A characterization of the AVF properties was carried out before and after surface treatment involving ATR-FTIR spectroscopy and SEM analysis. Surface morphology, thermal stability, water absorption capacity and rheological properties of both untreated and treated biocomposite samples were investigated. The study showed that the PHBHHx biocomposite/AVF treated with combined alkaline/organosilanes exhibited a better surface morphology resulting in a good fiber/matrix interfacial adhesion. Accordingly, an increase in complex viscosity, storage modulus and loss modulus was observed, whereas water absorption was reduced. Thermal stability remained almost unchanged except for the treated biocomposite with alkaline where this property decreased significantly. This study highlights the effectiveness of combined alkaline/organosilanes treatment of AVF over alkaline and organosilanes in PHBHHx biocomposites.

**Keywords:** PHBHHx; Aloe Vera fibers; biocomposites; fiber surface treatments

## 1. Introduction

In the last decade, lignocellulosic fibers reinforced biodegradable polymer composites attracted a great attention [1] because such new class of materials are promising candidates for replacing the synthetic polymer materials derived from fossil oil [2]. In this regard, polyhydroxyalkanoates (PHAs), which are aliphatic polyesters synthesized from bacteria under specific conditions [3], have been extensively investigated owing to their advantageous properties in many application fields involving mainly biomedical, food packaging, and agricultural [4]. Among the PHAs’ family, PHBHHx copolymer is considered as the third generation one, which is biodegradable and biocompatible possessing a lower melting temperature (~135 °C), a lower crystallinity index (~35–40%), and a wider window process than polyhydroxybutyrate (PHB) and poly(3-hydroxybutyrate-*co*-3-hydroxyvalerate) (PHBV) [5]. On the other hand, Aloe Vera fibers (AVF) offer a great deal of potential in engineering materials but unfortunately not enough investigated so far, in comparison

with lignocellulosic fibers [6]. Indeed only a very few studies were reported in literature on AVF, often dealing with properties characterization, surface modification and applications as fillers in polylactides (PLA) [7–9]. Therefore in this paper, the objective was to investigate the effect of various chemical surface treatments of Aloe Vera fibers on morphology and properties of PHBHHx biocomposites aiming to improve the matrix-filler compatibility and subsequently, their properties. AVF were subjected to alkaline treatment, organosilanes treatment and combined alkaline-organosilanes treatment and incorporated in PHBHHx matrix at filler content of 20 wt%.

## 2. Experiments

### 2.1. Materials

PHBHHx (11 wt% of hydroxyhexanoate) in pellets form was provided by Kaneka Corporation (Westerlo-Oevel, Belgium) under the grade Aonilex X151A.

Aloe Vera fibers (AVF) were extracted from leaves collected in the region of Bejaia (Algeria). The extraction procedure is described in the next Section 2.2.

Trimethoxy-octadecyl-silanes (TMOS) was purchased from Sigma Aldrich-(France).

Sodium hydroxyde (NaOH) was provided by Biochem-(United Kingdom).

### 2.2. Extraction Procedure and Chemical Composition of Aloe Vera fibers (AVF)

Aloe Vera fibers were extracted from the leaves using watter retting as described by Mannai et al. [10]: firstly, the leaves were washed out and cut into small pieces, then immersed in a thermostatically controlled water bath at 90 °C for 2 h. After this, AVF were removed and placed in a closed water container for 15–20 days. At the end, the fibers were washed several times and dried in an oven at 70° C overnight.

The chemical composition of AVF was determined using the analytical method reported in litterature [11,12] and the results are as follow: cellulose = 64.9 wt%, lignin = 4.1 wt%, hemicellulose = 25.1 wt% and extractives = 5.9 wt%. Density of AVF = 1.4325, which is consistent with the litterature [7].

### 2.3. Fiber Surface Treatments

#### 2.3.1. Alkaline Treatment

In order to eliminate the hemicellulose and partially the lignin, a treatment with NaOH was carried out according to the procedure reported in literature [7,13]. Initially, the fiber length was cut to ~3 mm and dried at 70 °C overnight. AVF were immersed in a NaOH solution at 5 wt% for 1 h, while the temperature was kept at 27 °C. After this, AVF were removed and washed several times with distilled water and once, with a solution of acetic acid at 2 wt% until reaching a neutral pH. The fibers were then dried at 70 °C until the mass stabilization.

#### 2.3.2. Organosilanes Treatment by TMOS

AVF surface treatment by TMOS was conducted according to the following procedure: AVF were sonicated in a mixture of water/ethanol (30/70 v/v) for 1 h. 2% of TMOS (w/w) were separately dissolved in a mixture of water/ethanol (70/70 v/v) for 1 h at pH = 4. The sonicated AVF were then soaked in the TMOS solution and kept under continuous stirring for 3 h at 25 °C [14,15]. AVF were filtered and dried in an oven at 110 °C for 12 h for completing the silanols groups condensation [12].

#### 2.3.3. Combined Alkaline-Organosilanes Treatment

AVF fibers were subjected to both alkaline and organosilane treatments as described above.

## 2.4. Preparation of PHBHHx/AVF Biocomposites

Before processing, PHBHHx and AVF were dried in a vacuum oven at 70 °C for 12 h to remove the moisture contained in the materials. PHBHHx/AVF biocomposites were prepared in a twin-screw micro-compounder, Model DSM Xplore(version 1.0-2005) at 145 °C and 50 rpm. AVF (before and after treatment) were incorporated into PHBHHx at loading ratio of 20 wt%. Table 1 summarizes the code and composition of the biocomposites formulations.

**Table 1.** Code and composition of neat PHBHHx and biocomposite formulations based on PHBHHx/AVF.

Sample Codes	PHBHHx (wt %)	AVF (wt %)	Designation
PHBHHx	100	-	Matrix
UNAVF	80	20	PHBHHx/Untreated AVF
ALAVF	80	20	PHBHHx/alkaline treated AVF
SiAVF	80	20	PHBHHx/organosilanes treated AVF
ALSiAVF	80	20	PHBHHx/combined alkaline and organosilanes treated AVF

## 2.5. Characterization Techniques

Fracture surface morphology of the biocomposite samples were observed by using a Jeol JSM-6031 scanning electron microscope. Prior to any observation, the fracture surface of the biocomposite samples were coated with a thin gold layer by means of a Polaron sputtering apparatus.

TGA analysis was performed in a thermal analyzer (Setaram TGDTA92-10) with a heating rate of 10 °C/min under nitrogen atmosphere from 20 to 600 °C. The average weight samples was almost 10 mg and three replicates were performed for each sample.

Rheological measurements were carried out by an Anton PaarMCR301 rheometer. The samples were dried at 60 °C for 24 h before testing. The experiments were done at 150 °C using a 25 mm parallel plate system. The disks were equilibrated for 4 min before the gap was set to the testing position of 0.95 mm. The limit of the linear viscoelastic regime was determined by performing a strain sweep at 1 Hz. A strain of 0.5%, corresponding to the linear viscoelastic domain, was chosen to perform dynamic measurements over a frequency range from 0.01 to 100 Hz.

Water absorption percentage was determined by measuring the difference between the weight at initial time and the constant final weight of the sample at a given time according to ASTM D570-98 (2018) standard method. The samples were dried in a vacuum oven at 70 °C overnight, cooled in a desiccator, and immediately weighed using a four-digital balance. The conditioned samples were then immersed in distilled water at room temperature. The samples were removed regularly, blotted to eliminate excess water on the surface and weighted. The percentage of water absorption (WA %) was calculated according to Equation (1) [16].

$$W_A(\%) = \frac{m_t - m_0}{m_0} \times 100\% \quad (1)$$

where  $W_A$  is the water absorption in %,  $m_t$  is the sample weight after a given immersion time, and  $m_0$  is the initial weight sample before immersion. The average scatter around the mean value was  $\pm 0.1\%$ .

## 3. Results

### 3.1. Morphological Analysis of PHBHHx/AVF before and after Surface Treatment

Figure 1a–e, shows SEM micrographs of the fracture surface of neat PHBHHx, PHBHHx/untreated AVF, PHBHHx/alkaline-treated AVF, PHBHHx/organosilanes-treated AVF, and PHBHHx/combined alkaline-organosilanes treated AVF biocomposites, respectively. In Figure 1a, the fracture surface of neat PHBHHx is homogenous and compact. Figure 1b relative to PHBHHx/UNAVF shows the presence of some aggregates with some fibers are pulled out from the

matrix indicating the lack of adhesion. Furthermore some surface defects such as craters and microvoids are visible. For the PHBHHx/ALAVF biocomposite, the fracture surface shown in Figure 1c, exhibits some microscopic holes and cavities in the matrix where ALAVF are randomly distributed. Figure 1d shows clearly an improved surface morphology of PHBHHx/SiAVF biocomposite, resulting in a reduction of the number and size of aggeragtes. Figure 1e displays the fracture surface morphology of PHBHHx/ALSiAVF biocomposite, which is characterized by a regular and homogenous surface having less defects and fibers pullouts compared with other PHBHHx biocomposites.

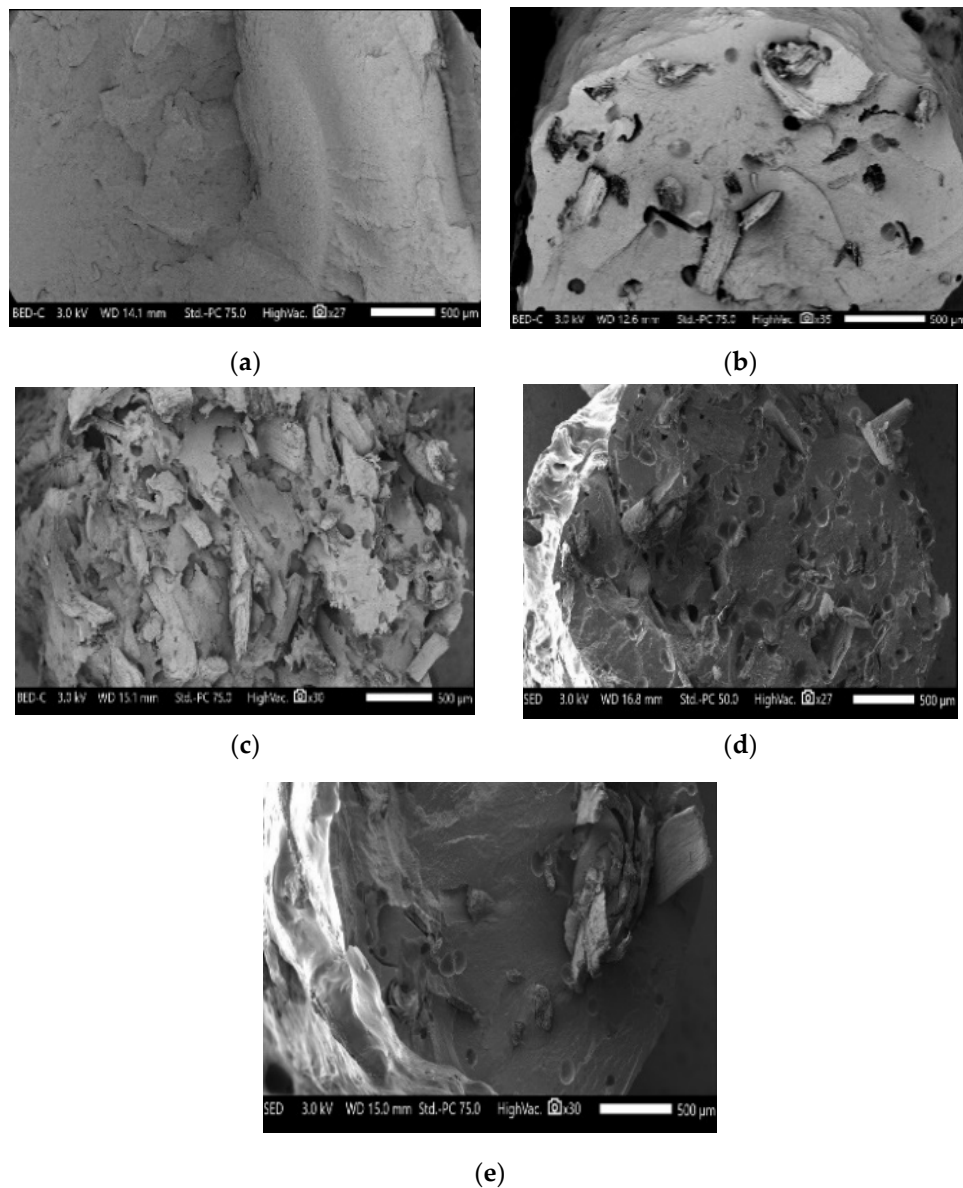


**Figure 1.** SEM micrographs of: (a) neat PHBHHx, (b) PHBHHx/UAVF, (c) PHBHHx/ATAVF, (d) PHBHHx/STAVF, (e) PHBHHx/ALSTAVF.

### 3.2. Rheological Measurements

Table 2 summarizes the values of complex viscosity ( $\eta^*$ ), storage modulus ( $G'$ ) and loss modulus ( $G''$ ) of neat PHBHHx and various PHBHHx/AVF biocomposites, recorded at 0.01 Hz. A significant effect of AVF on the rheological properties is observed. Indeed,  $\eta^*$  increases from 4100 Pa.s for the neat PHBHHx to more than 105 Pa.s for the PHBHHx/UNAVF biocomposite, even more for the treated samples indicating the restriction of chain mobility of PHBHHx. This behavior is more pronounced for the biocomposite filled with ALSiAVF. Similar trend is also observed for  $G'$  and  $G''$ .

**Table 2.** The values of complex viscosity ( $\eta^*$ ) storage modulus ( $G'$ ) and loss modulus ( $G''$ ) of PHBHHx and PHBHHx/AVF before and after treatment recorded at 0.01 Hz.

Sample	$\eta^*$ (Pa.S)	$G'$ (Pa)	$G''$ (Pa)
PHBHHx	4100	6.18	258
PHBHHx/UNAVF	111,000	5100	4760
PHBHHx/ALAVF	835,000	50,500	14,000
PHBHHx/SiAVF	228,000	9610	10,600
PHBHHx/ALSiAVF	1,240,000	66,500	40,800

### 3.3. TGA Data

Thermal stability of various PHBHHx/AVF biocomposites before and after treatments was carried out by TGA and the results compared to those of neat PHBHHx. Table 3 shows the temperature values of  $T_{10}$  and  $T_{50}$  corresponding to 10 and 50% mass loss, while  $T_{mdr}$  is the temperature corresponding to the maximum degradation rate. The % residue at 600 °C is also given in Table 3. The incorporation of AVF in PHBHHx results in a slight decrease in thermal stability of the biocomposite samples whatever the type of fiber. Indeed, it can be noticed that  $T_{10}$ ,  $T_{50}$  and  $T_{mdr}$  shift to lower temperatures, being however more pronounced for the biocomposite filled with alkaline treated fibers.

**Table 3.** TGA data of neat PHBHHx and various PHBHHx/AVF biocomposites before and after fiber surface treatment.

Samples	$T_{10}$ (°C)	$T_{50}$ (°C)	$T_{mdr}$ (°C)	Char Yield (%)
PHBHHx	$280 \pm 0.5$	$294 \pm 1.8$	$295 \pm 1.1$	$0.2 \pm 0.05$
PHBHHx/UNAVF	$274 \pm 0.8$	$288 \pm 1.9$	$288 \pm 0.8$	$4.2 \pm 0.6$
PHBHHx/ALAVF	$260 \pm 0.7$	$274 \pm 1.7$	$276 \pm 0.9$	$4.3 \pm 0.4$
PHBHHx/SiAVF	$278 \pm 0.4$	$293 \pm 1.3$	$293 \pm 0.3$	$1.9 \pm 0.1$
PHBHHx/ALSiAVF	$277 \pm 0.2$	$289 \pm 1.1$	$292 \pm 0.3$	$1.6 \pm 0.1$

### 3.4. Water Absorption (WA)

Figure 2 shows the water uptake of neat PHBHHx and PHBHHx/AVF biocomposites before and after surface treatment. All WA curves exhibit similar trend, which is characterized by a fast increase of WA during the first 24 h of immersion before reaching the saturation. As expected, PHBHHx has the lowest water absorption, while the PHBHHx/ALAVF biocomposite shows the highest one.

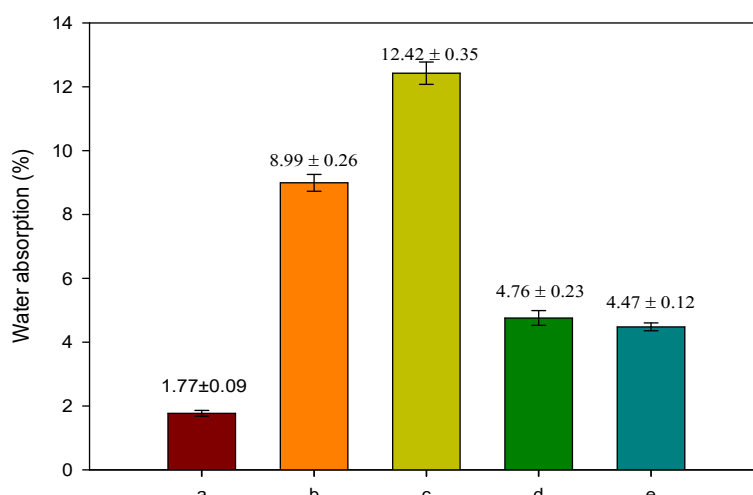


**Figure 2.** Water absorption (%) at saturation (a) neat PHBHHx, (b) PHBHHx/UNAVF, (c) PHBHHx/ALAVF, (d) PHBHHx/SiAVF and (e) PHBHHx/ALSiAVF.

#### 4. Discussion

Morphological observations shown in Figure 1b indicate the formation of UNAVF aggregates in PHBHHx matrix, some fiber pullouts and microvoids. This behavior is a characteristic of incompatible system, which results in a low interfacial adhesion between natural fibers and hydrophobic polymer matrix [17]. However, the combined alkaline organosilanes treatment of AVF leads to a better morphology resulting in enhancement of the fibers wettability and subsequently to strong interactions between AVF and PHBHHx. Indeed, according to Orue et al. [14] the grafted TMOS on AVF surface promotes the interfacial adhesion due to its bifunctional structure.

Rheological measurements show a significant increase in  $\eta^*$  at a lower frequency (0.01 Hz), which is attributed to a hindring effect on the chains mobility after adding AVF. Similar behaviors are reported for  $G'$  and  $G''$  which indicate a good interfacial bonding between PHBHHx and AVF, however being more pronounced for the PHBHHx biocomposite filled with ALSiAVF. This is consistent with the data reported by Komal et al. [18].

TGA show that T10, T50 and Tmdr shift to lower temperatures after adding AVF. This could be explained as a result of the moisture contained in the materials [19] and also to a slight alteration of the cellulose structure during the chemical treatment [20].

PHBHHx shows the lowest water uptake due to its hydrophobic nature. Whereheas, the PHBHHx/ALAVF shows the highest percentage owing to the alkaline treatment, which causes the surface roughness and fibrillation of the fibers, thus increasing the number of reactive sites [21]. The rest of PHBHHx biocomposites have intermediate values. PHBHHx/UNAVF has the highest WA % due to the hydrophilic nature of the cellulosic fibers [22], whereas PHBHHx/SiAVF and PHBHHx/ALSiAVF) exhibit lower values resulting from the presence of silanol groups that are chemically adsorbed onto the fiber, thus preventing fiber swelling [23,24].

#### 5. Conclusions

In the current study, the effect of several surface treatments on Aloe Vera fibers and their impact on morphology and properties of PHBHHx biocomposites prepared by melt compounding, was investigated. Morphological data showed the importance of such treatments to improve the dispersion of AVF in the matrix by avoiding the formation of filler aggregates and enhancing the filler-matrix interfacial adhesion. Furthermore, the biocomposite with combined alkaline organosilanes treated AVF displayed better thermal stability, rheological properties and lower water uptake in comparison with the other biocomposites.

**Author Contributions:** C.I. performed the experiments and wrote the paper; M.K. conceived and designed the experiments; and N.D., I.Z. and S.B. analyzed and validated the data. All authors have read and agreed to the published version of the manuscript.

**Acknowledgments:** the authors are grateful to Campus France through Tassili PHC program No 19MDU204 for its financial support in this collaborative project.

**Conflicts of Interest:** The authors declare no conflict of interest.

#### Abbreviations

The following abbreviations are used in this manuscript:

PHBHHx	poly(3-hydroxybutyrate- <i>co</i> -3-hydroxyhexanoate)
Aloe Vera Fiber	AVF
ATR-FTIR	Attenuated total reflectance-Fourier transform infrared spectroscopy
SEM	Scanning Electron Microscopy
TMOS	Trimethoxy-octadecyl-silanes
UNAVF	Untreated Aloe Vera fiber
ALAVF	Alkaline treated Aloe Vera Fiber
SiAVF	Organosilanes treated Aloe Vera Fiber
ALSiAVF	combined alkaline organosilanes treated fiber
TGA	Thermogravimetric analysis

## References

1. Bharath, K.N.; Basavarajappa, S. Applications of biocomposite materials based on natural fibers from renewable resources: A review. *Sci. Eng. Compos. Mater.* **2016**, *23*, 123–133, doi:10.1515/secm-2014-0088.
2. Murphy, C.A.; Collins, M.N. Microcrystalline cellulose reinforced polylactic acid biocomposite filaments for 3D printing. *Polym. Compos.* **2016**, *39*, 1311–1320, doi:10.1002/polym.24069.
3. Kennouche, S.; Le Moigne, N.; Kaci, M.; Quantin, J.-C.; Caro-Bretelle, A.-S.; Delaite, C.; Lopez-Cuesta, J.-M. Morphological characterization and thermal properties of compatibilized poly (3-hydroxybutyrate-co-3-hydroxyvalerate)(PHBV)/poly (butylene succinate)(PBS)/halloysite ternary nanocomposites. *Eur. Polym. J.* **2016**, *75*, 142–162.
4. Ivorra-Martinez, J.; Verdu, I.; Fenollar, O.; Sánchez-Nacher, L.; Balart, R.; Quiles-Carrillo, L. Manufacturing and Properties of Binary Blend from Bacterial Polyester Poly(3-hydroxybutyrate-co-3-hydroxyhexanoate) and Poly(caprolactone) with Improved Toughness. *Polymers* **2020**, *12*, 1118, doi:10.3390/polym12051118.
5. Raza, Z.A.; Abid, S.; Banat, I.M. Polyhydroxyalkanoates: Characteristics, production, recent developments and applications. *Int. Biodeterior. Biodegradation* **2018**, *126*, 45–56, doi:10.1016/j.ibiod.2017.10.001.
6. Faruk, O.; Bledzki, A.K.; Fink, H.-P.; Sain, M. Biocomposites reinforced with natural fibers: 2000–2010. *Prog. Polym. Sci.* **2012**, *37*, 1552–1596, doi:10.1016/j.progpolymsci.2012.04.003.
7. Balaji, A.N.; Nagarajan, K.J. Characterization of alkali treated and untreated new cellulosic fiber from Saharan aloe vera cactus leaves. *Carbohydr. Polym.* **2017**, *174*, 200–208, doi:10.1016/j.carbpol.2017.06.065.
8. Chaitanya, S.; Singh, I. Novel Aloe Vera fiber reinforced biodegradable composites—Development and characterization. *J. Reinf. Plast. Compos.* **2016**, *35*, 1411–1423, doi:10.1177/0731684416652739.
9. Chaitanya, S.; Singh, I. Ecofriendly treatment of aloe vera fibers for PLA based green composites. *Int. J. Precis. Eng. Manuf. Technol.* **2018**, *5*, 143–150, doi:10.1007/s40684-018-0015-8.
10. Mannai, F.; Elhleli, H.; Ammar, M.; Passas, R.; Elaloui, E.; Moussaoui, Y. Green process for fibrous networks extraction from Opuntia (Cactaceae): Morphological design, thermal and mechanical studies. *Ind. Crop. Prod.* **2018**, *126*, 347–356, doi:10.1016/j.indcrop.2018.10.033.
11. Li, S.; Xu, S.; Liu, S.; Yang, C.; Lu, Q. Fast pyrolysis of biomass in free-fall reactor for hydrogen-rich gas. *Fuel Process. Technol.* **2004**, *85*, 1201–1211, doi:10.1016/j.fuproc.2003.11.043.
12. Varma, A.K.; Mondal, P. Physicochemical Characterization and Pyrolysis Kinetic Study of Sugarcane Bagasse Using Thermogravimetric Analysis. *J. Energy Resour. Technol.* **2016**, *138*, 052205, doi:10.1115/1.4032729.
13. Joyyi, L.; Thirmizir, M.Z.A.; Salim, M.S.; Han, L.; Murugan, P.; Kasuya, K.-I.; Maurer, F.H.; Arifin, M.I.Z.; Sudesh, K. Composite properties and biodegradation of biologically recovered P(3HB- co -3HHx) reinforced with short kenaf fibers. *Polym. Degrad. Stab.* **2017**, *137*, 100–108, doi:10.1016/j.polymdegradstab.2017.01.004.
14. Orue, A.; Jauregi, A.; Unsuain, U.; Labidi, J.; Eceiza, A.; Arbelaitz, A. The effect of alkaline and silane treatments on mechanical properties and breakage of sisal fibers and poly (lactic acid)/sisal fiber composites. *Compos. Part A Appl. Sci. Manuf.* **2016**, *84*, 186–195.
15. Georgopoulos, P.; Kontou, E.; Georgousis, G. Effect of silane treatment loading on the flexural properties of PLA/flax unidirectional composites. *Compos. Commun.* **2018**, *10*, 6–10, doi:10.1016/j.coco.2018.05.002.
16. Wu, C.-S. Assessing biodegradability and mechanical, thermal, and morphological properties of an acrylic acid-modified poly (3-hydroxybutyric acid)/wood flours biocomposite. *J. Appl. Polym. Sci.* **2006**, *102*, 3565–3574.
17. Berthet, M.-A.; Gontard, N.; Angellier-Coussy, H. Impact of fibre moisture content on the structure/mechanical properties relationships of PHBV/wheat straw fibres biocomposites. *Compos. Sci. Technol.* **2015**, *117*, 386–391, doi:10.1016/j.compscitech.2015.07.015.
18. Komal, U.K.; Lila, M.K.; Singh, I. PLA/banana fiber based sustainable biocomposites: A manufacturing perspective. *Compos. Part B Eng.* **2020**, *180*, 107535, doi:10.1016/j.compositesb.2019.107535.
19. Vandi, L.-J.; Chan, C.M.; Werker, A.; Richardson, D.; Laycock, B.; Pratt, S. Extrusion of wood fibre reinforced poly(hydroxybutyrate-co-hydroxyvalerate) (PHBV) biocomposites: Statistical analysis of the effect of processing conditions on mechanical performance. *Polym. Degrad. Stab.* **2019**, *159*, 1–14, doi:10.1016/j.polymdegradstab.2018.10.015.
20. Rachini, A.; Le Troedec, M.; Peyratout, C.; Smith, A. Comparison of the thermal degradation of natural, alkali-treated and silane-treated hemp fibers under air and an inert atmosphere. *J. Appl. Polym. Sci.* **2009**, *112*, 226–234, doi:10.1002/app.29412.

21. Li, X.; Tabil, L.G.; Panigrahi, S. Chemical Treatments of Natural Fiber for Use in Natural Fiber-Reinforced Composites: A Review. *J. Polym. Environ.* **2007**, *15*, 25–33, doi:10.1007/s10924-006-0042-3.
22. Kaci, M.; Djidjelli, H.; Boukerrou, A.; Zaidi, L. Effect of wood filler treatment and EBAGMA compatibilizer on morphology and mechanical properties of low density polyethylene/olive husk flour composites. *Express Polym. Lett.* **2007**, *1*, 467–473, doi:10.3144/expresspolymlett.2007.65.
23. Hydrophobic Treatment of Natural Fibers and Their Composites—A Review. Available online: [https://scholar.google.fr/scholar?hl=fr&as\\_sdt=0%2C5&q=Hydrophobic+treatment+of+natural+fibers+and+their+composites%2E2%80%94A+review&btnG=](https://scholar.google.fr/scholar?hl=fr&as_sdt=0%2C5&q=Hydrophobic+treatment+of+natural+fibers+and+their+composites%2E2%80%94A+review&btnG=) (accessed on 30 September 2020).
24. Gogoi, R.; Tyagi, A.K. Surface Modification of Jute Fabric by Treating with Silane Coupling Agent for Reducing Its Moisture Regain Characteristics. *J. Nat. Fibers* **2019**, *1*–10, doi:10.1080/15440478.2019.1658252.

**Publisher's Note:** MDPI stays neutral with regard to jurisdictional claims in published maps and institutional affiliations.



© 2020 by the authors. Licensee MDPI, Basel, Switzerland. This article is an open access article distributed under the terms and conditions of the Creative Commons Attribution (CC BY) license (<http://creativecommons.org/licenses/by/4.0/>).